Structure of a λ-Type Bence-Jones Protein at 6-Å Resolution†

Allen B. Edmundson,* Marianne Schiffer, Kathryn R. Ely, and Mical K. Wood‡

ABSTRACT: An electron density map at 6-Å resolution has been calculated for a λ-type Bence-Jones protein. Mersalyl-sodium and *o*-chloromercuriphenol were used to prepare isomorphous derivatives. The mersalyl ion was located in one major and two secondary sites, while *o*-chloromercuriphenol was found in two positions. The most distinctive features of the electron density map were the large volumes occupied by solvent, which formed well-defined boundaries with the protein. The asymmetric unit, a dimer of molecular weight 46,000, was represented by two globular modules differing in size and structure. The modules were partially separated by a crevice, but continuous electron density between the two was also observed. The differences in size and shape were too large for the modules to correspond to identical monomers. Instead, the results support the conclusion that the amino- and carboxyl-terminal parts of the Bence-Jones monomer fold independently into regions having little affinity for each other, but substantial affinity for homologous parts in a second chain. The division of the polypeptide chains into independently folded regions appeared to be asymmetric, with the region bridging the amino and carboxyl halves mainly contained in the larger module.

Functional IgG antibody molecules are composed of two light (mol wt 22,000–23,000) and two heavy chains (mol wt 50,000–55,000) linked by interchain disulfide bonds.[1] Free light chains excreted into the urine in patients with multiple myeloma are called Bence-Jones proteins (Edelman and Gally, 1962), the presence of which is pathognomonic of the disease. There are two principal antigenic classes (κ and λ) of light chains, and the proteins may exist as monomers or dimers (Milstein, 1965; Cohen and Milstein, 1967). The Bence-Jones protein (Mcg) described in the present article is a λ-type dimer in which the two identical polypeptide chains are covalently linked by a disulfide bond between penultimate half-cystine residues.

For each antigenic type and species, the amino acid sequences of light chains can be divided into variable N-terminal (V) and relatively constant C-terminal (C) halves (Hilschmann and Craig, 1965; Titani *et al.*, 1965). The V part is associated with both the antigenic specificity of light chains (Edelman and Gall, 1969; Milstein and Pink, 1970) and the characteristic thermal properties (Solomon and McLaughlin, 1969) of Bence-Jones proteins. In antibody molecules the C part of the light chain is usually bonded to the heavy chain.

The V and C halves of light chains can be examined separately after limited proteolysis of the polypeptide chain in the "switch" region between the two parts (Solomon and McLaughlin, 1969; Solomon *et al.*, 1970; Karlsson *et al.*, 1969; Björk *et al.*, 1971; Schramm, 1971). Optical rotatory dispersion and circular dichroism studies show that the conformational changes accompanying this cleavage are minimal (Björk *et al.*, 1971). Hydrodynamic measurements (Karlsson *et al.*, 1969) and calculations of "average hydrophobicities" (Welscher, 1969) support the hypothesis that both V and C parts have compact globular structures. One of the objectives in examining the 6-Å electron density map is to evaluate the possibility of such independently folded structures in light chains.

Materials and Methods

Crystallization of the Bence-Jones Protein. The protein was precipitated from urine by the addition of solid ammonium sulfate to 90% saturation. The precipitate was dissolved in 0.1 M Tris-HCl (pH 8.0) and the protein was crystallized at 4° by dialysis against deionized water. After purification by recrystallization under the same conditions, the protein behaved as a single component on columns of Sephadex G-100 and in the ultracentrifuge (Schiffer *et al.*, 1970; Edmundson *et al.*, 1971).

Crystals for diffraction were grown at pH 6.2 in 1.6 to 1.9 M ammonium sulfate, which was also 0.1 M in phosphate. Addition of the ammonium sulfate to a solution containing 20–30 mg of protein/ml produced a gel, which acted to keep the centers of crystallization apart and thereby increase the yield of suitable crystals (*i.e.*, 0.4–0.7 mm wide, 1.0–1.5 mm long). The crystals had 32 symmetry, with the long axis corresponding to *c*. A photograph of the crystals is shown in Figure 1.

The symmetry of the diffraction pattern [$\bar{3}m$, twofold normal to $(11\bar{2}0)$] and the systematic extinctions observed on precession photographs (*i.e.*, $00l$ absent unless $l = 3n$) indicated that the space group was trigonal $P3_121$ or its enantiomorph $P3_221$ (no. 152 and 154: Henry and Lonsdale, 1965). The unit cell dimensions were $a = 72.3 \pm 0.2$ and $c = 185.9 \pm 0.6$ Å, and the asymmetric unit was the dimer (mol wt = 46,000). The fractional volume of solvent (V_{solv}) in the crystals was calculated (Matthews, 1968) to be 0.60.

Preparation of Isomorphous Derivatives. The derivatives were prepared with 0.01 M mersalylsodium and 0.001 M *o*-chloromercuriphenol, made up in buffered 1.9 M ammonium sulfate (pH 6.2). Crystals were soaked in these solutions for 4–6 weeks.

† From the Division of Biological and Medical Research, Argonne National Laboratory, Argonne, Illinois 60439. *Received December 8, 1971.* This work was supported by the U. S. Atomic Energy Commission. A preliminary account of this work was presented by M. S. at the summer meeting of the American Crystallographic Association at Ames, Iowa, Aug 15–20, 1971.

* To whom to address correspondence.

‡ Present address: Oakland Veterans Administration Hospital, Pittsburgh, Pa.

[1] For reviews of the subject, see *Gamma Globulins, Proc. Nobel Symp. 3*, 1967; *Cold Spring Harbor Symp. Quant. Biol. 32*, 1967; *FEBS Symp. 15*, 1969.

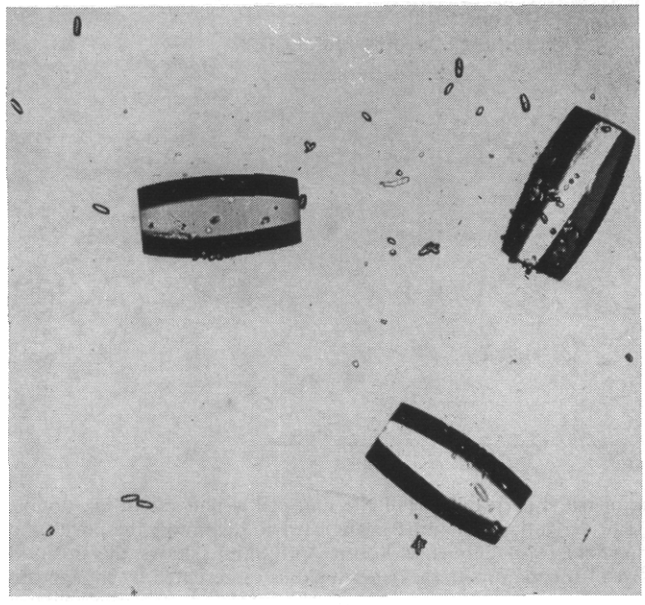

FIGURE 1: Photograph of crystals of the Bence-Jones protein.

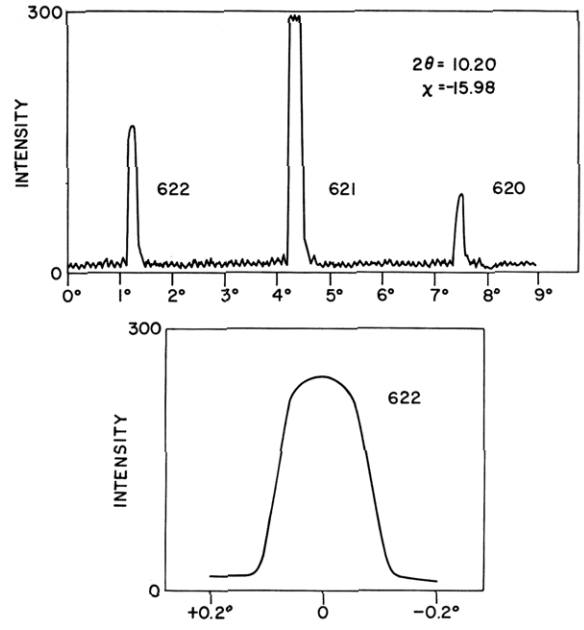

FIGURE 2: Reflections resolved with the diffractometer on the basis of differences in their ϕ angles. The crystal was cut to a length of 0.5 mm and the c axis was oriented across the quartz capillary. The 2θ and χ values of the three reflections, with successively increasing l indices, were for 620, $2\theta = 10.18°$ and $\chi = -16.02°$; for 621, $2\theta = 10.20°$ and $\chi = -15.99°$; and for 622, $2\theta = 10.22°$ and $\chi = -15.93°$. Since they were nearly identical in the three cases, the 2θ and χ angles were set to average values of 10.20 and $-15.98°$ before the ϕ scan was begun. The ϕ scan of the 622 reflection is shown in more detail in the lower panel of the figure. The widths of such peaks at the half-height ranged from about 0.12 to 0.15° in different crystals.

Collection of Data. Data were collected with a Picker diffractometer, controlled by an IBM 1131A computer (Mueller *et al.*, 1968). Nickel-filtered, Cu Kα radiation (43 kV, 16 mA) from a standard focus tube set for a take-off angle of 4° was used in conjunction with a Picker X-ray generator. ω step scans, with six steps at intervals of 0.03°, were employed (Wyckoff *et al.*, 1967), and the observed number of counts for each reflection was taken as the largest sum of three adjacent measurements. Each set of 6-Å data for the native protein or derivative was collected from one crystal.

To achieve resolution of reflections differing only in their l indices (*i.e.*, parallel to the 186 Å c axis), it was necessary to take advantage of the inherent low angular dispersion of the diffracted beam parallel to the ω circle of the diffractometer. Accordingly, crystals were cut at right angles to c to give a length of ~0.5 mm, and the fragments were placed with c across the capillary. The c^* axis was aligned perpendicular to the ϕ axis.

The separations achieved for three adjacent reflections with increasing l indices are illustrated by the ϕ scan in Figure 2. With the 2θ and χ angles set to average values, these reflections were well resolved on ϕ. An example of the *least* favorable case in the 6-Å sphere is shown in Figure 3. Because of the systematic extinctions, only every third reflection is present in the 00l row. Therefore, the reflections closest together are the high order 01l reflections, which are separated along the 2θ and ϕ directions. Reflections 0,1,24 and 0,1,25 differ by 0.48° in 2θ and 0.24° in ϕ. A combined 2θ and ϕ step scan at intervals of 0.04° on 2θ and 0.02° on ϕ revealed that the two reflections were completely resolved. Moreover, with ϕ set at the value for the 0,1,25 reflection, a 2θ step scan over the range for both the 0,1,24 and 0,1,25 reflections showed the expected peak for the latter and only base line for the former reflection.

ϕ scans such as the one shown at the bottom of Figure 2 indicate that the peaks were generally symmetrical, with the width ranging from 0.12 to 0.15° at the half-height. The mosaic spread, as determined for the 900 reflection ($\chi = 90°$) at a take-off angle of 1° with the receiving aperture fully opened, averaged 0.12° at the base of the peak.

Measured intensities were corrected for background, Lorentz, polarization, and absorption factors and for radiation damage. Background corrections were calculated from the averaged results of three radial scans between lattice points at 0.5° intervals on 2θ. The absorption correction was calculated from a ϕ scan of a polar reflection at 5° intervals. A linear correction for radiation damage was determined from averaged intensity changes in four general reflections measured after every 100 reflections.

Data collected by the present method have been repro-

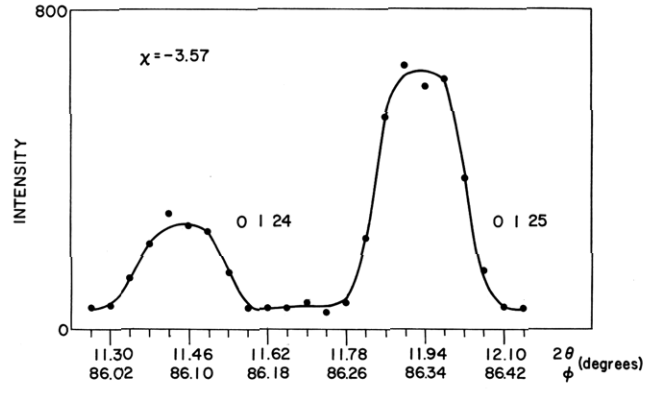

FIGURE 3: Combined 2θ and ϕ step scan of the 0, 1, 24 and 0, 1, 25 reflections in a test of the least favorable case for resolution of reflections in the 6-Å sphere. The 2θ and ϕ values used to center each reflection were for 0, 1, 24, $2\theta = 11.46°$ and $\phi = 86.10°$; for 0, 1, 25, $2\theta = 11.94°$ and $\phi = 86.34°$. The crystal to detector distance was 52 cm; the take-off angle was 4°; and the receiving aperture was 2 × 4 mm.

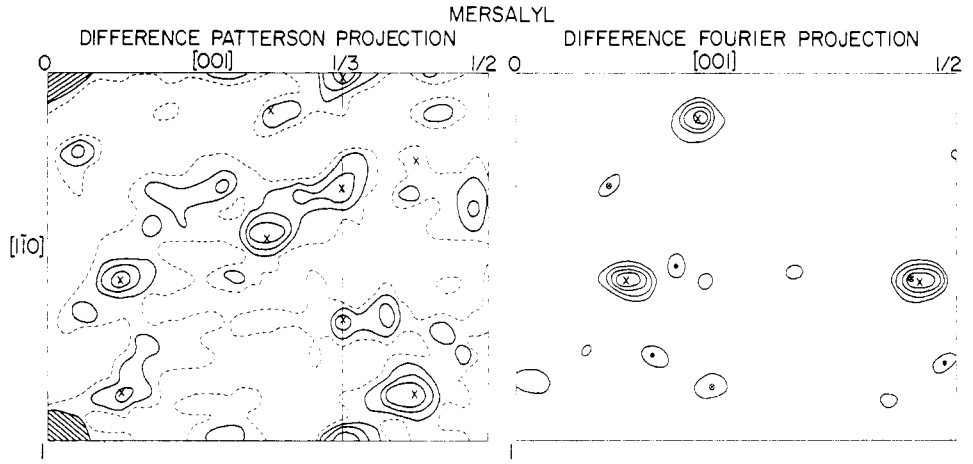

FIGURE 4: A difference Patterson projection along the [110] axis for the mersalyl derivative. Half the unit cell is illustrated. Six double-weight and three single-weight Harker peaks are expected for a single-site derivative. The nine peaks used to determine the position of the major mersalyl site are indicated by X's. In the second panel, the final [110] difference Fourier projection shows the positions of the two minor sites (designated by dots and circled X's), as well as that of the major site (X's). Each site is represented by three peaks, corresponding to the three asymmetric units in half the unit cell. Both maps are on an arbitrary scale. In the Patterson map, the height of the origin peak is 1000; contours are drawn at intervals of 50; and the zero contours are represented by dashed lines. The contour interval on the Fourier map is 200, with the zero contours omitted.

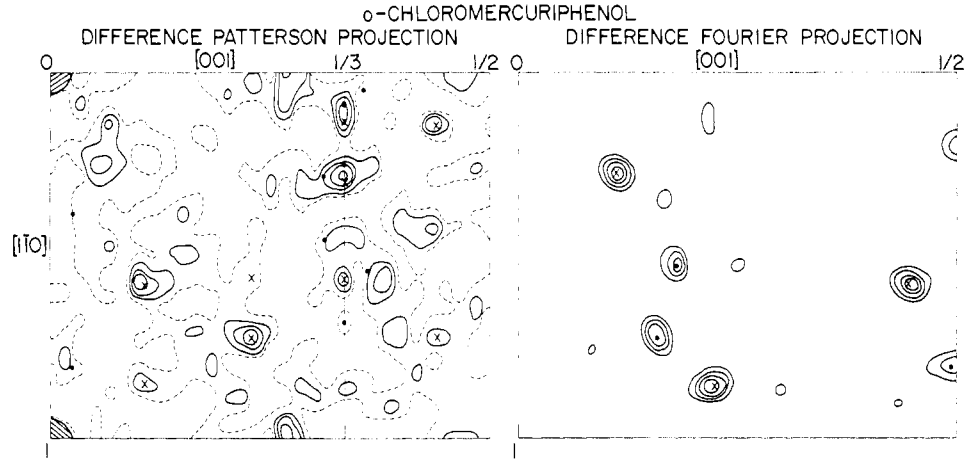

FIGURE 5: Difference Patterson and difference Fourier projections for the *o*-chloromercuriphenol derivative. The peaks for the first site are indicated by X's; those for the second site are marked with dots.

ducible in different crystals to the extent that $\Sigma|\Delta F|/\Sigma F = 0.06$. The absorption corrections ranged from 0 to 40%, while the decay corrections were 5–9% in crystals of native proteins and 3–18% in the derivatives after 30-hr exposure to the X-ray beam.

Results

Location of Heavy-Atom Positions. The principal site occupied by the mersalyl ion was located in a [110] difference Patterson projection, the only centric projection in the $P3_121$ space group (see Figure 4). For one heavy atom in each asymmetric unit, six double-weight and three single-weight Harker peaks are expected in this projection for one-half the unit cell.

The nine peaks used to define the principal mersalyl site are marked with X's in Figure 4. The difference Patterson projection for the *o*-chloromercuriphenol derivative was more difficult to interpret, but one consistent set of peaks was identified (see peaks denoted by X's in Figure 5).

Using centric data, the heavy-atom positions, occupancies, and isotropic temperature factors of the two mercurial derivatives were refined together by alternate cycles of phase determination and least-squares refinement (Dickerson *et al.*, 1961, 1968). After refinement the improved phases were used to calculate the [110] difference Fourier projections, which indicated the positions of the major sites, as well as two minor sites for the mersalyl derivative (see Figure 4) and one secondary site for the *o*-chloromercuriphenol derivative (see Figure 5). Each site is represented by three peaks, corresponding to the three asymmetric units in half the unit cell.

The *calculated* positions of the Harker peaks for the second *o*-chloromercuriphenol site are marked with dots on the difference Patterson projection in Figure 5. The cross vectors between the two heavy atoms all fell within positive regions on the Patterson map.

When the secondary sites were included in the refinement procedure, the *R* factors for centric reflections decreased from 0.67 to 0.55 in the mersalyl derivative and from 0.65 to 0.46 in the *o*-chloromercuriphenol derivative (see Table I). The figure of merit increased from 0.54 to 0.66.

TABLE I: Final Heavy-Atom Parameters.[a]

Derivative	Site	x	y	z	B	A	E	R_K (All)	R_C (Centric)	R_F (Centric)
Mersalyl	1	0.440	0.872	0.129	56.9	717	394	0.082	0.55	0.19
	2	0.440	0.154	0.107	8.5	120				
	3	0.209	0.452	0.155	5.8	85				
o-Chloromercuriphenol	1	0.420	0.142	0.115	9.4	319	398	0.077	0.46	0.23
	2	0.195	0.476	0.156	12.5	240				

[a] B = temperature factor; A = occupancy; E = lack of closure error on an arbitrary scale; average protein F = 3040 on this scale. $R_K = [\Sigma|F_{PH,obsd} - F_{PH,calcd}|]/\Sigma F_{PH,obsd}$, $R_C = [\Sigma|F_{H,obsd} - F_{H,calcd}|]/\Sigma F_{H,obsd}$, and $R_F = \Sigma|F_{PH} - F_P|/\Sigma F_P$, where F = structure factor amplitude; P = protein; H = heavy atom; PH = protein plus heavy atom. Figure of merit = 0.66.

Using all data, the heavy-atom parameters were further refined in four cycles.[2] The coordinates of the mercurials and the other results of the refinement are presented in Table I. The results indicate that the secondary mersalyl sites are situated close to the *o*-chloromercuriphenol positions. Examination of the electron density map reveals that all heavy-atom sites are located on or near the surface of the protein molecule.

Electron Density Map. The electron density map was calculated with "best" phases (Blow and Crick, 1959), and with the observed structure factors weighted by the figure of merit. Sections perpendicular to the a^* axis were computed at intervals of $0.04a$, $0.17b$, and $0.008c$, from 0 to 1 in the x and y directions and from 0 to 0.5 in the z direction. The map was on an arbitrary scale, with the highest peak set at a value of 999. Contouring was performed at intervals of 200, the zero contours being omitted. The contours were plotted from the computer printout directly onto Plexiglas sheets. Photographs of representative sections of the electron density map are shown in Figure 6. Density considered to be part of one asymmetric unit is designated with marker dots and stars. A model of the asymmetric unit, constructed of free-foamed styrofoam to a scale of 1.45 Å to 1 cm, is also illustrated in Figure 6.

The most outstanding features of the map are the large volumes of space occupied by solvent. Examples of clearly defined boundaries between protein and solvent can be seen in Figure 6a.

The asymmetric unit consists of two dissimilar modules of electron density. These modules are marked with dots (type 1) and stars (type 2) in Figure 6a. The modules are partially separated by a crevice, which extends from the top of the model shown in Figure 6 (panels c–e) to the segments of continuous density between the two modules (see Figure 6d and the junction between the dots and stars in Figure 6a). The estimated chain length of module 1 is ~1.3–1.4 times that of module 2, and the distribution of electron density is also different. Together, modules 1 and 2 correspond to the Bence-Jones dimer.

Because of the close intermolecular packing of symmetrically related modules (see Figure 6b), we considered different combinations of type 1 and type 2 modules before building the model of the dimer. The combination chosen gives the maximum amount of electron density between modules and a particle length (~78 Å) similar to that (~75 Å) found for a Bence-Jones dimer by low-angle X-ray scattering measurements (Holasek *et al.*, 1963).

Discussion

The results indicate that the Bence-Jones dimer is composed of two globular regions which are unequal in size and structure. Because of these differences, the regions cannot be monomers. Instead, our results provide strong evidence that the amino- and carboxyl-terminal parts of an immunoglobulin light chain fold independently into regions having little affinity for each other, but substantial affinity for homologous parts in a second chain. At the present resolution it is not possible to determine which module contains the carboxyl parts, but the identification in higher resolution maps should be facilitated by the fact that the two parts are connected by an interchain disulfide bond.

In light chain monomers there are two *intra*chain disulfide bonds, each connecting a loop of approximately 60 residues.[1] The loops are found in homologous positions in the V and C halves and are separated by 48 residues in λ chains. An N-terminal segment of 20–21 residues and a C-terminal segment of 19 residues lie outside the loops. The size of the small module in the crystal structure is sufficient to accommodate one disulfide loop and one terminal segment from each chain of the dimer, but the segments bridging the V and C parts have to be located mainly in the larger module.

These connecting segments contain peptide bonds which can be cleaved in some light chains to produce stable V and C fragments. The products released from the Mcg protein by the action of trypsin and pepsin are currently being examined to determine which bonds are most susceptible to hydrolysis. Attempts are also being made to crystallize the fragments.

The sensitivity of light chains to limited proteolysis is consistent with the hypothesis that the segments linking compact regions of the Bence-Jones proteins are composed of extended chains (Karlsson *et al.*, 1969). The flexibility conferred on two interacting monomers by such extended chains may help explain the absence of crystallographic and noncrystallographic twofold axes of symmetry between the Mcg monomers in the crystal. Local twofold axes within the modules may become apparent at higher resolution.

Comparison of amino acid sequences have indicated homologies between the light and heavy chains of immunoglobu-

[2] The program for calculation of phases and refinements of heavy-atom parameters was kindly supplied by Dr. R. E. Dickerson. It was modified at Argonne for use with the $P3_121$ space group.

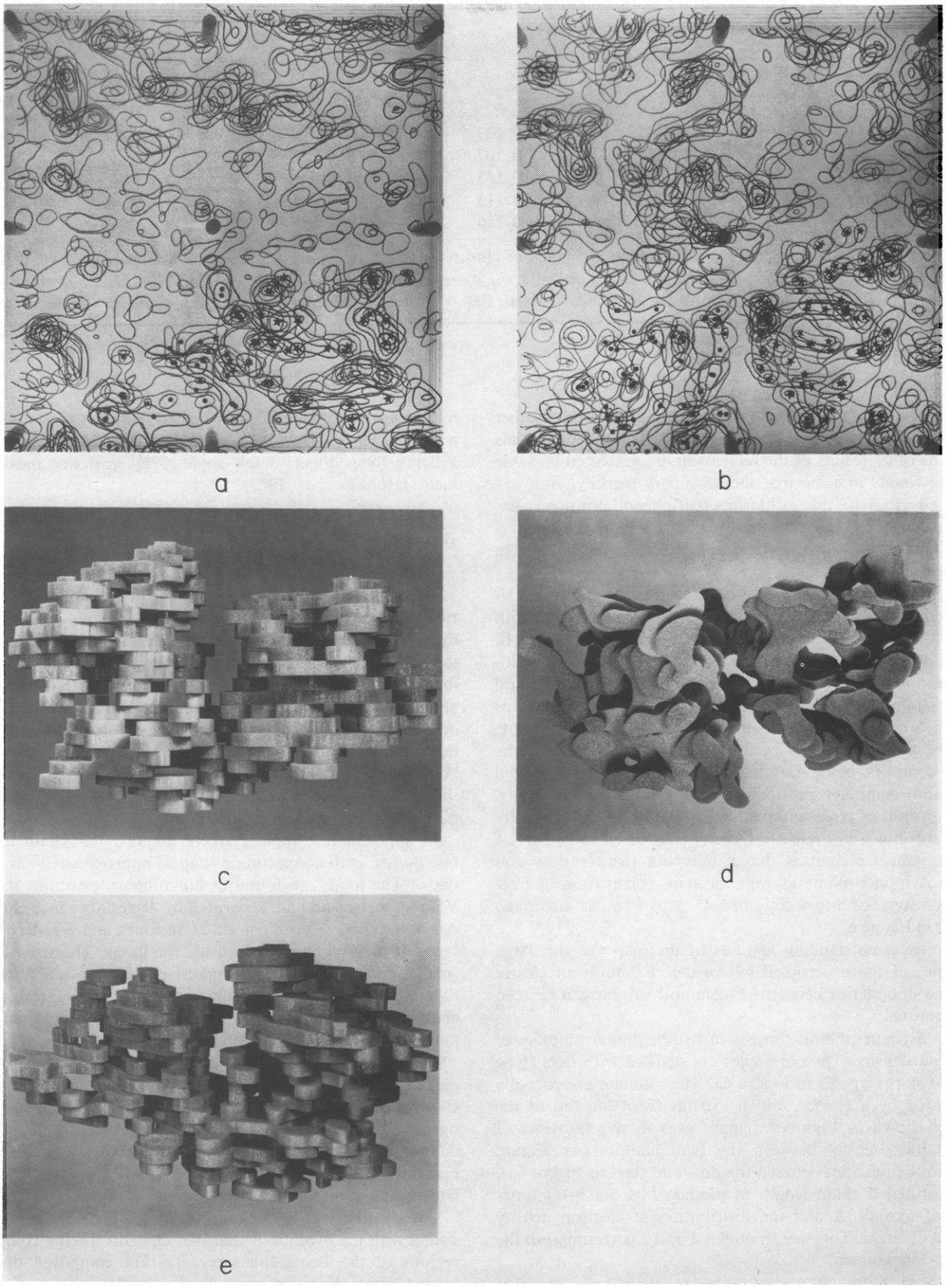

FIGURE 6: Photographs of sections of the 6-Å electron density map and the styrofoam model of the asymmetric unit. (a) Sections normal to a^* axis, from $x = 0$ to 0.24, with y the ordinate and z the abscissa in each section. The lowest contour is one-fifth the maximum, and zero contours are omitted. In the center of the photograph note the region of low density corresponding to solvent. These superposed sections contain the regions of continuous electron density between the modules which we consider part of one asymmetric unit (see junction between marker dots and stars). (b) Sections from $x = 0.28$ to 0.52. The module (1) of electron density marked with dots is centered at $x = 0.4$, $y = 0.67$, and $z = 0.17$, while the module (2) designated with stars is centered at $x = 0.36$, $y = 0.5$, and $z = 0.33$. (c) Styrofoam model of the asymmetric unit, viewed approximately at right angles to the line joining the centers of modules 1 and 2. Module 1 is on the left. (d) View of the model in the same orientation as the electron density map above it. (e) Back view of the model. Module 1 is on the right.

lins.[1] In view of the chemical homologies and the similarities in size of a Bence-Jones dimer and a functional antigen-binding fragment (Fab: a disulfide-linked complex of a light chain and the amino half of a heavy chain; see Poljak *et al.*, 1971), it will be interesting to see if the crystal structure of the Mcg Bence-Jones dimer resembles that of an Fab fragment at low resolution.

Acknowledgments

We thank H. F. Deutsch for his continued interest; D. Cripps and H. F. Deutsch for obtaining the urine specimens from which the Bence-Jones protein was prepared; O. Smithies for advice and encouragement; our colleagues K. D. Hardman and C. F. Ainsworth for their suggestions and support; G. Svihla for photographing the crystals; F. W. Markley, W. R. Cole, B. S. Kotula, W. J. Eisler, and D. A. LeBuis for aid and advice in the design and construction of the styrofoam model; and H. C. Watson for his hospitality and guidance to A. E. during an extended visit in his laboratory.

References

Björk, I., Karlsson, F. A., and Berggård, I. (1971), *Proc. Nat. Acad. Sci. U. S. 68*, 1707.

Blow, D. M., and Crick, F. H. C. (1959), *Acta Crystallogr. 12*, 794.

Cohen, S., and Milstein, C. (1967), *Advan. Immunol. 7*, 1.

Dickerson, R. E., Kendrew, J. C., and Strandberg, B. E. (1961), *Acta Crystallogr. 14*, 1188.

Dickerson, R. E., Weinzierl, J. E., and Palmer, R. A. (1968), *Acta Crystallogr., Sect. B 24*, 997.

Edelman, G. M., and Gall, W. E. (1969), *Annu. Rev. Biochem. 38*, 415.

Edelman, G. M., and Gally, J. A. (1962), *J. Exp. Med. 116*, 207.

Edmundson, A. B., Schiffer, M., Wood, M. K., Hardman, K. D., Ely, K. R., and Ainsworth, C. F. (1971), *Cold Spring Harbor Symp. Quant. Biol. 36*, 427.

Henry, N. F. M., and Lonsdale, K., Ed. (1965), International Tables for X-ray Crystallography, Vol. I, 2nd ed, Birmingham, England, Kynoch Press.

Hilschmann, N., and Craig, L. C. (1965), *Proc. Nat. Acad. Sci. U. S. 53*, 1403.

Holasek, A., Kratky, O., Mittlebach, P., and Wawra, H. (1963), *J. Mol. Biol. 7*, 321.

Karlsson, F. A., Peterson, P. A., and Berggård, I. (1969), *Proc. Nat. Acad. Sci. U. S. 64*, 1257.

Matthews, B. W. (1968), *J. Mol. Biol. 33*, 491.

Milstein, C. (1965), *Nature (London) 205*, 1171.

Milstein, C., and Pink, J. R. L. (1970), *Progr. Biophys. Mol. Biol. 21*, 209.

Mueller, M. H., Heaton, L., and Amiot, L. (1968), *Res. Develop. 19*, 34.

Poljak, R. J., Amzel, L. M., Avey, H. P., Becka, L. N., Goldstein, D. J., and Humphrey, R. L. (1971), *Cold Spring Harbor Symp. Quant. Biol. 36*, 421.

Schiffer, M., Hardman, K. D., Wood, M. K., Edmundson, A. B., Hook, M. E., and Ely, K. R. (1970), *J. Biol. Chem. 245*, 728.

Schramm, H. J. (1971), *Hoppe-Seyler's Z. Physiol. Chem. 352*, 1134.

Solomon, A., and McLaughlin, C. L. (1969), *J. Biol. Chem. 244*, 3393.

Solomon, A., McLaughlin, C. L., Wei, C. H., and Einstein, J. R. (1970), *J. Biol. Chem. 245*, 5289.

Titani, K., Whitley, Jr., E., Avogardo, L., and Putnam, F. W. (1965), *Science 149*, 1090.

Welscher, H. D. (1969), *Int. J. Protein Res. 1*, 253.

Wyckoff, H. W., Doscher, M., Tsernoglou, D., Inagami, T., Johnson, L. N., Hardman, K. D., Allewell, N. M., Kelly, D. M., and Richards, F. M. (1967), *J. Mol. Biol. 27*, 563.